Published in final edited form as:
J Neurochem. 2008 September ; 106(6): 2395–2409. doi:10.1111/j.1471-4159.2008.05582.x.

Occludin oligomeric assembly at tight junctions of the blood-brain barrier is disrupted by peripheral inflammatory hyperalgesia

Gwen McCaffrey[*], **Melissa J. Seelbach**[*], **William D. Staatz**[*], **Nicole Nametz**[*], **Carolyn Quigley**[*], **Chris R. Campos**[*], **Tracy A. Brooks**[†], and **Thomas P. Davis**[*,†]

[*]*Department of Medical Pharmacology, University of Arizona College of Medicine, Tucson, Arizona, USA*

[†]*Bio5 Institute, Tucson, Arizona, USA*

Abstract

Tight junctions (TJs) at the blood-brain barrier (BBB) dynamically alter paracellular diffusion of blood-borne substances from the peripheral circulation to the CNS in response to external stressors, such as pain, inflammation, and hypoxia. In this study, we investigated the effect of λ-carrageenan-induced peripheral inflammatory pain (i.e., hyperalgesia) on the oligomeric assembly of the key TJ transmembrane protein, occludin. Oligomerization of integral membrane proteins is a critical step in TJ complex assembly that enables the generation of tightly packed, large multiprotein complexes capable of physically obliterating the interendothelial space to inhibit paracellular diffusion. Intact microvessels isolated from rat brains were fractionated by detergent-free density gradient centrifugation, and gradient fractions were analyzed by sodium dodecyl sulfate—polyacrylamide gel electrophoresis/Western blot. Injection of λ-carrageenan into the rat hind paw produced after 3 h a marked change in the relative amounts of oligomeric, dimeric, and monomeric occludin isoforms associated with different plasma membrane lipid raft domains and intracellular compartments in endothelial cells at the BBB. Our findings suggest that increased BBB permeability (i.e., leak) associated with λ-carrageenan-induced peripheral inflammatory pain is promoted by the disruption of disulfide-bonded occludin oligomeric assemblies, which renders them incapable of forming an impermeant physical barrier to paracellular transport.

Keywords

blood-brain barrier; density gradient; inflammatory pain; occludin; tight junction; trafficking

The blood-brain barrier (BBB) is anatomically comprised of approximately 20 m^2 of endothelial cells (per 1.3 kg brain) that line the vascular microvessels of the brain to form a physical, metabolic, and immunologic barrier between the CNS and the peripheral circulation (Reese and Karnovsky 1967; de Boer and Gaillard 2007). Breach of the BBB (i.e., leak) exposes the brain's fragile micro-environment to potentially harmful substances in the periphery, and may result in a loss of brain homeostasis characterized by nutritional and ionic imbalances, impaired neuronal signaling, improper delivery of therapeutic pharmaceuticals, serum protein extravasation, and cerebral edema leading to increased intracranial pressure and death (Petty and Lo 2002; Hawkins and Davis 2005; Zlokovic 2008).

How BBB integrity is modulated by pain and/or inflammation is a research priority (Neuwelt *et al*. 2008). Pain afflicts more than 76 million Americans each year, causing tremendous

Address correspondence and reprint requests to Gwen McCaffrey, PhD, Department of Medical Pharmacology, College of Medicine, University of Arizona, 1501 N. Campbell Ave, Tucson, AZ 85745, USA. E-mail: gwenm@email.arizona.edu.

suffering and costing an estimated $100 billion dollars in medical treatments and loss of productivity (http://www.painfoundation.org). Moreover, BBB dysfunction adversely affects the course of numerous CNS and non-CNS diseases and pathologies associated with pain and/or inflammation including Alzheimer's disease, arthritis, diabetes, multiple sclerosis, ischemic stroke, and peripheral inflammatory pain (Petty and Lo 2002; Hawkins and Davis 2005; Desai *et al*. 2007; Pan and Kastin 2007; Forster 2008; Kaur and Ling 2008; Zlokovic 2008).

Pain is a complex phenomenon involving responses from the immune system and the CNS as well as activation of the hypothalamic—pituitary—adrenal axis (Wolka *et al*. 2003). All categories of pain (acute, subchronic, and chronic) can be initiated by a painful stimulus or inflammagen that elicits both a peripheral innate immune response and a CNS response. The peripheral innate immune response to injury involves the rapid production and local release of inflammatory mediators at the site of injury or inflammation. The CNS response to peripheral inflammatory pain involves glia activation, *de novo* synthesis of proinflammatory cytokines and growth factors, and exaggerated pain transmission (hyperalgesia) (Watkins *et al*. 1995; Watkins and Maier 2000, 2005; Wieseler-Frank *et al*. 2005a,b). Inflammatory mediators produced in the CNS may affect endothelial cells at the BBB through the abluminal face, and systemic inflammatory mediators may affect endothelial cells through the luminal face (Watkins *et al*. 1995; Andersson 2005; Hansson and Zugner 2005).

Disruption of paracellular permeability at the BBB during peripheral inflammatory pain has been demonstrated in our laboratory using three different experimental models (formalin, λ-carrageenan, and complete Freund's adjuvant) (Huber *et al*. 2001,2006;Hau *et al*. 2004; Brooks *et al*. 2005,2006;Seelbach *et al*. 2007). Recently, we demonstrated the use of a neutral pH, detergent-free, isosmotic OptiPrep density gradient method to fractionate intact cerebral microvessels to isolate oligomeric occludin and claudin-5 within the context of their normal plasma membrane environment (McCaffrey *et al*. 2007). Oligomerization of integral membrane proteins such as occludin and claudin-5 is an essential architectural feature of the tight junction (TJ) multiprotein complexes that form between cerebral microvascular endothelial cells to physically inhibit paracellular diffusion at the BBB. Pioneering *in vitro* work by Blasig *et al*. (2006) demonstrated the self-association of occludin and claudin-5 within plasma membranes of the same cell and the trans-interaction between claudin-5 molecules of adjacent cells (Piontek *et al*. 2008), elegantly establishing a molecular model for homophilic and heterophilic interaction between claudins at the TJ (Krause *et al*. 2008). The transmembrane protein, occludin, critically important for barrier function at the BBB, functions at the TJ as both a structural and a signaling protein (Dobrogowska and Vorbrodt 2004;Harhaj and Antonetti 2004;Vorbrodt and Dobrogowska 2004;Feldman *et al*. 2005;Hawkins and Davis 2005;Gonzalez-Mariscal *et al*. 2008;Paris *et al*. 2008;Vandenbroucke *et al*. 2008). Within the occludin primary sequence there is a stretch of approximately 200 amino acids that shows statistical similarity to the myelin and lymphocyte (MAL) and related proteins for vesicle trafficking and membrane link (MARVEL) domain (Sanchez-Pulido *et al*. 2002). MARVEL domains, characterized by an M-shaped topology comprised of a four transmembrane-helix architecture with cytoplasmic N- and C-terminal regions, have a putative role in cholesterol-rich membrane apposition events such as biogenesis of vesicular transport carriers or membrane fusion. Occludin and the claudins, TJ transmembrane proteins of dissimilar primary sequence but similar membrane topology, are incorporated within cholesterol-enriched regions of the plasma membrane (Hendset *et al*. 2006) and interact through their extracellular loops with homologous segments on apposing endothelial cell membranes to form the seal that restricts paracellular diffusion (Lacaz-Vieira *et al*. 1999;Wen *et al*. 2004;Krause *et al*. 2008;Piontek *et al*. 2008). Attached to the C-termini of occludin is zonula occludens-1 (ZO-1), the primary cytoplasmic accessory TJ protein responsible for anchoring TJ transmembrane protein oligomeric assemblies to the underlying actin cytoskeleton (Furuse *et al*. 1994). Occludin interacts with a variety of signaling, regulatory or vesicle trafficking proteins

including c-Yes (Chen and Lu 2003), the regulatory (p85) subunit of phosphatidylinositol 3-kinase (Sheth *et al.* 2003), transforming growth factor beta receptors I and II (Barrios-Rodiles *et al*. 2005;Ozdamar *et al*. 2005), caveolin (Nusrat *et al*. 2000b), protein kinase C-zeta, connexin-26 (Nusrat *et al.* 2000a;Feldman *et al.* 2005), Rab13 (Morimoto *et al.* 2005), and 33 kDa Vamp-associated protein (Lapierre *et al*. 1999). Numerous reports associate occludin's phosphorylation state with TJ regulation (Hirase *et al*. 2001;Kago *et al*. 2006;Persidsky *et al*. 2006;Stamatovic *et al*. 2006;McKenzie and Ridley 2007;Seth *et al*. 2007;Yamamoto *et al*. 2008). Moreover, many studies have associated oxidative stress with occludin phosphorylation and trafficking and TJ function (Kevil *et al*. 2000;Rao *et al*. 2002;Fischer *et al*. 2005;Krizbai *et al.* 2005;DeMaio *et al.* 2006), and affirmed a protective role for anti-oxidants in preventing changes in barrier integrity (Meyer *et al*. 2001;Xu *et al*. 2007).

In this study, we investigate the effect of peripheral inflammatory hyperalgesia on occludin oligomeric assembly at TJs of the BBB *in vivo*. We show that there is a significant reduction in 'TJ-associated' oligomeric (> 150 kDa) occludin within microvascular endothelial cell plasma membrane lipid rafts at the BBB within 3 h of intraplantar injection of 3% λ-carrageenan into the right hind paw of female Sprague—Dawley rats. Our data are not inconsistent with the hypothesis that disulfide bond formation/reduction between occludin oligomeric assemblies of apposing cells contributes importantly to the dynamic nature of TJ multiprotein complexes and represents a potential target of therapeutic manipulation of TJ paracellular permeability.

Materials and methods

Chemicals and reagents

OptiPrep was purchased from Accurate Chemical (Westbury, NY, USA). EDTA-free Complete Proteinase Inhibitor was obtained from Roche (Indianapolis, IN, USA). Criterion XT (10% Bis-Tris) gels, 20× 3-morpholinopropanesulfonic acid running buffer, 4× XT sample loading buffer, 20× XT reducing agent, tris(2-carboxyethyl)phosphine hydrochloride (TCEP), and Precision Plus pre-stained molecular weight markers were obtained from Bio-Rad (Hercules, CA, USA). Polyvinylidene difluoride (PVDF) (0.45 μm) and Western Lightning Chemiluminescence Reagent Plus were purchased from Perkin Elmer (Waltham, MA, USA). Blue autoradiography film was bought from Genesee Scientific (San Diego, CA, USA). Bicinchoninic acid protein assay reagent and albumin standard were purchased from Pierce (Rockford, IL, USA). All other chemicals and reagents were obtained from either Fisher Scientific (Fairlawn, NJ, USA) or Sigma (St. Louis, MO, USA).

Antibodies

The mouse monoclonal antibody against ZO-1 (33–9100) and the rabbit polyclonal antibody against occludin C-terminus (71–1500) were purchased from Zymed (South San Francisco, CA, USA). The goat polyclonal antibody against Rab13 (sc-30374) and the rabbit polyclonal antibody against nucleoporin (sc-25523) were obtained from Santa Cruz Biotechnology (Santa Cruz, CA, USA). The mouse monoclonal antibodies against coatomer subunit beta (β-COP) (G 6160) and caveolin-1 (610406) were purchased from Sigma and BD Transduction Laboratories (San Jose, CA, USA), respectively.

Animals and treatments

Female Sprague—Dawley rats (250–300 g) were purchased from Harlan Sprague—Dawley (Indianapolis, IN, USA), housed under standard 12 h light/12 h dark conditions, and given food and water *ad libitum*. Animals weighing 250–300 g were randomly assigned to each treatment group, and all treatment protocols were approved by the University of Arizona Institutional Animal Care and Use Committee, and abided by National Institutes of Health guidelines. Rats

were gently restrained in the conscious state, and each received an injection (100 μL, s.c.) of either λ-carrageenan (3% diluted in 0.9% saline) or saline (0.9%, vehicle control) into the plantar surface of the right hand paw. Assessment of paw edema and thermal hyperalgesia was carried out as previously described (Seelbach *et al*. 2007). *In situ* brain perfusion was performed as per Huber *et al*. (2001).

Microvessel isolation

Animals were anesthetized with sodium pentobarbital (64 mg/kg; i.p.) and subjected to transcardiac perfusion with 0.9% saline for 2 min. Following decapitation, brains were removed and cerebral microvessels isolated as previously described (McCaffrey *et al*. 2007).

Confocal microscopy

Rat cerebral microvessels (isolated as described above) were spread onto glass microscope slides and immunostained as previously described (McCaffrey *et al*. 2007). Images were acquired using an LSM 510 confocal laser-scanning microscope under an 63× oil-immersion objective and data were analyzed by LSM 5 software (Carl Zeiss Inc., Thornwood, NY, USA).

Microvessel fractionation

Rat cerebral microvessels (isolated as described above) were fractionated by an adaptation of the detergent-free method of Macdonald and Pike (2005), as previously described (McCaffrey *et al*. 2007). The protein content of microvessel homogenates were determined by bicinchoninic acid protein assay prior to density gradient centrifugation to ensure that equal protein amounts of microvessel homogenate (adjusted to equal volumes) were layered beneath OptiPrep gradients.

SDS-PAGE and Western blot analysis

Protein samples and pre-stained molecular weight markers were separated by sodium dodecyl sulfate—polyacrylamide gel electrophoresis (SDS—PAGE) on 10% Bis-Tris Criterion XT precast gels using 3-morpholinopropanesulfonic acid buffer, electrophoretically transferred to PVDF membranes using Genie Electroblotters (Idea Scientific, Minneapolis, MN, USA), probed, and analyzed as previously described (McCaffrey *et al*. 2007). Typically, protein samples were mixed with XT sample loading buffer (containing 1× XT reducing agent TCEP) and heated for 10 min at 70 °C. In particular instances, protein samples were supplemented with 10% SDS and 10 mM 1,2-ethanedithiol (EDT) and heated for 10 min at 100 °C. Antibody specificity was routinely verified by control experiments in which the primary antibody was omitted and only secondary antibody was used. In addition, specificity of the rabbit polyclonal antibody directed against the C-terminus of occludin (Zymed 71–1500) was affirmed by control experiments in which the primary antibody was either the mouse monoclonal antibody against the C-terminus of occludin (Zymed 33–1500) or the non-specific mouse IgG1 control antibody (Zymed 08–6599).

Statistical analysis

Data are expressed as mean ± SE. Paw volume and paw withdrawal data were analyzed using Student's *t*-test. Significance was defined as $p < 0.05$.

Results

Characterization of λ-carrageenan pain model

The λ-carrageenan model of peripheral inflammatory pain uses injection of λ-carrageenan into the plantar surface of the rat hind paw to elicit localized inflammation and associated hyperalgesia (Huber *et al*. 2002; Ibuki *et al*. 2003; Seelbach *et al*. 2007). Paw edema, a marker

of the inflammatory response, is measured by plesmythmography. Thermal hyperalgesia, a measure of inflammation-induced pain the experimental animal perceives by way of nociception, was assessed using the Hargreaves radiant heat test (Hargreaves *et al*. 1988). Injection of 100 μL of 3% λ-carrageenan solution in the right hind paw produced significant paw swelling within 3 h (Fig. 1a). Paw swelling was not observed within the contralateral paw of λ-carrageenan-injected animals nor in the hind paw of saline-injected controls. A significant decrease in paw withdrawal latency was observed for the λ-carrageenan-injected paw (Fig. 1b). Paw latency changes were not observed within the contralateral paw of λ-carrageenan-injected animals, nor in the hind paw of saline-injected controls. Shown in Fig. 1c are data on the permeability of sucrose. These data provide evidence that λ-carrageenan causes a significant increase in paracellular sucrose permeability. Collectively, these data confirmed that our model of λ-carrageenan treatment produced peripheral inflammatory hyperalgesia specifically localized to the right hind paw, and significantly altered BBB function.

Effect of λ-carrageenan on TJ protein localization in isolated cerebral microvessels

To provide a global assessment of changes in TJ transmembrane and accessory protein localization that would complement subcellular fractionation data, intact cerebral microvessels were analyzed by confocal microscopy following immunostaining for occludin and ZO-1 (Fig. 2). Hind paw injection of λ-carrageenan slightly decreased the overall intensity of occludin staining in isolated microvessels. Interestingly, no evident change in immunostaining of the TJ accessory protein ZO-1 was observed. Collectively, these data indicate that following 3 h of inflammatory peripheral hyperalgesia, there appeared to be a modest alteration in the distribution of occludin within endothelial cells at the BBB. This change in occludin localization was not mirrored by a corresponding change in ZO-1 localization.

Characterization of OptiPrep density gradient fractionation of cerebral microvessels

To investigate λ-carrageenan-induced modulation of TJ multiprotein complexes at the BBB *in vivo*, cerebral microvessel TJ structures were isolated within the context of their native lipid raft environment. Intact microvessels obtained from brains of control- and λ-carrageenan-injected animals were fractionated using a density gradient centrifugation method designed to separate plasma membrane lipid rafts from non-raft membranous structures (Macdonald and Pike 2005; McCaffrey *et al*. 2007). Fractionation of cerebral microvessel homogenates prepared from brains from saline-and λ-carrageenan-injected animals produced gradients with nearly identical density profiles (Fig. 3a). The average fraction density (ρ, calculated from refractive indices) increased linearly across gradients between 1.038 g/mL (top of gradient) and 1.168 g/mL (bottom of gradient). Protein profiles for density gradients prepared using cerebral microvessel homogenates obtained from saline- and λ-carrageenan-injected animals were similar, with low-density fractions containing significantly less protein than that found at the bottom of the gradients (Fig. 3b).

Density gradients were screened for the location of raft and non-raft markers using the ‘constant volume’ (versus the ‘constant protein’) mode to ensure accurate estimation of proteins associated with low density, low protein, and lipid-enriched membrane domains (Macdonald and Pike 2005; Rudajev *et al*. 2005). Because equal protein aliquots of brain microvessel homogenates (prepared from saline- and λ-carrageenan-injected animals) were fractionated, and density profiles of gradients were routinely determined following centrifugation to ensure quality of fractionation, the amount of a particular protein marker contained within equal volumes of same-density fractions from different gradients could be compared by SDS—PAGE/Western blot. By loading equal volumes of each gradient fraction, as opposed to equal protein, artificial overestimation of proteins within lipid rafts was avoided. Pairs of SDS—PAGE gels of gradient samples were routinely electrophoresed (one gel loaded with gradient samples 1–15 from saline-injected animals, and the other gel loaded with corresponding

gradient samples from the λ-carrageenan-injected animals). Additionally, both gels were blotted side-by-side to the same PVDF membrane to ensure that blotting and antibody probing were identical for the two treatment groups.

Western blots of gradient fractions probed for plasma membrane lipid raft markers (Rab13 and caveolin-1), the Golgi membrane protein, β-COP, and the nuclear membrane protein nucleoporin confirmed the separation of plasma membrane lipid raft domains (fractions 5 to 10; ρ = 1.068 to 1.120 g/mL) from intracellular membranous components (fractions 11 to 15; ρ = 1.132 to 1.168 g/mL) (Fig. 3c). Microvessels isolated from brains of saline-injected animals revealed strongest staining of Rab13 in fraction 7 (ρ = 1.081 g/mL), the low density plasma membrane lipid raft domain previously characterized as co-localizing with oligomeric assemblies of the key TJ transmembrane proteins, occludin and claudin-5 (McCaffrey *et al*. 2007). Peripheral inflammatory hyperalgesia promoted a distinct reduction in the amount of Rab13 associated with plasma membrane lipid rafts, with the greatest decrease occurring in fraction 7. Similar to Rab13, higher molecular weight forms of the scaffolding protein caveolin-1 (72 and 89 kDa) stained prominently in plasma membrane lipid raft fractions 7 and 8, with significant staining also in fractions of higher density (9,10) and lower density (5,6). The effect of λ-carrageenan was to eliminate the presence of the higher 89 kDa form of caveolin-1 in fraction 7. Moreover, the 72 kDa isoform was also detectably decreased. λ-Carrageenan treatment also reduced the amount of low molecular weight (LMW) forms of caveolin-1 in non-raft domains. In contrast to the lipid raft markers, λ-carrageenan treatment did not cause noticeable changes in distribution of the Golgi marker, β-COP, or the nuclear membrane marker, nucleoporin. These non-raft markers prominently stained in fractions 12–15, at the bottom of the gradient. Collectively, these data confirm that cerebral microvessels isolated from animals with λ-carrageenan-induced peripheral inflammatory hyperalgesia may be successfully fractionated by neutral pH, detergent-free OptiPrep density gradient centrifugation to identify changes in distribution of TJ-associated proteins within plasma membrane lipid raft domains. Decreased association of Rab13 and the 72- and 89-kDa oligomeric forms of the scaffolding protein, caveolin-1, with the ‘TJ-associated’ low density plasma membrane domain (fraction 7, ρ = 1.081 g/mL) suggest that remodeling of these lipid rafts has occurred which may adversely affect the integrity of TJ transmembrane protein complexes.

λ-Carrageenan modulates occludin association with plasma membrane lipid rafts

The effect of peripheral inflammatory hyperalgesia on the integrity of TJ multiprotein complexes was investigated by focusing on the relative distribution of occludin between different plasma membrane lipid raft domains and intracellular compartments in endothelial cells at the BBB. Occludin trafficking was analyzed by SDS—PAGE/Western blot of fractions obtained from OptiPrep density gradient fractionation of cerebral microvessels isolated from brains from saline- and λ-carrageenan-injected animals. Using an antibody directed to the C-terminus of occludin (Zymed 71–1500), a complex array of oligomeric (> 150 kDa), dimeric (*c*. 110–120 kDa), monomeric (53–65 kDa), and LMW (37–35 kDa, 25 kDa) occludin isoforms were detected in gradient fractions from both saline- and λ-carrageenan-injected animal groups (Fig. 4a). Because gradient fractions were treated with the hydrophilic reducing agent, TCEP, in the presence of 2% SDS (10 min, 70 °C) prior to electrophoresis, the oligomeric and dimeric occludin isoforms represent ‘TCEP-resistant’ (TCEP-R) protein structures containing disulfide bonds within hydrophobic regions (McCaffrey *et al*. 2007). Monomeric and LMW occludin isoforms may represent components of higher molecular weight occludin isoforms that were attached either by disulfide bonds accessible to TCEP or by non-covalent interactions sensitive to SDS. Alternatively, these monomeric and LMW forms of occludin may have not been associated with higher molecular weight structures in either lipid raft or non-raft locations.

To aid the analysis of occludin isoform distribution within lipid raft and non-raft regions, the band density for each isoform was calculated as a percentage of the sum of band densities for that particular isoform across the gradient, and corresponding histograms for each occludin isoform were prepared (Fig. 4b). The majority of TCEP-R occludin oligomer detected in both saline- and λ-carrageenan-injected animals was found within plasma membrane lipid raft domains (fractions 5–10). In contrast, approximately equal amounts of TCEP-R occludin dimer (*c*. 100–120 kDa) were detected in both lipid raft and non-raft locations, suggesting that an equillibrium may exist between plasma membrane and cytoplasmic stores of this building block dimer. In saline-injected animals, 65% of raft-associated TCEP-R occludin oligomer was concentrated in the 'TJ-associated' low density plasma membrane lipid raft domain (fraction 7, ρ = 1.081 g/mL). Twenty-seven percent of TCEP-R occludin oligomer was detected in fraction 8, associated with plasma membrane lipid raft domains of higher density (ρ = 1.105 g/mL), and only minor amounts of this high molecular isoform could be detected in fractions 9, 10, 13, and 14 (ρ = 1.108 to 1.161 g/mL). Taken together, these data affirm the importance of the lipid raft environment in the establishment and maintenance of higher order TCEP-R oligomeric occludin structures. The presence of TCEP-R occludin dimer in non-raft domains indicates that the plasma membrane lipid raft environment is not required for either the formation or maintenance of hydrophobic disulfide bond(s) between monomeric subunits to form dimeric structures. The association of 92% of the total amount of TCEP-R oligomeric occludin with only two lipid raft fractions (7 and 8), combined with the preferential association of approximately two-thirds of detectable isoform with fraction 7 (the fraction of comparatively lowest density), suggests that occludin oligomeric assemblies arise from successive remodeling of occludin-containing lipid rafts. Lipid raft remodeling involving the incorporation or exclusion of different protein and lipid components to generate more structured environments of increasingly lower density would accompany increased packing and oligomerization of occludin isoforms until a lipid raft of unique lipid/protein composition and structural occludin oligomeric integrity is generated.

Injection of λ-carrageenan caused an approximate 20% decrease in total oligomeric occludin protein band density and disrupted the preferential association of the majority of TCEP-R occludin oligomers with the low density 'TJ-associated' plasma membrane lipid rafts present in fraction 7. Of the total amount of TCEP-R oligomer detected in the case of λ-carrageenan-treated animals, only 35% remained in fraction 7, whereas 52% and 9% were detected in fractions 8 and 10, respectively. In addition to TCEP-R oligomers, other occludin isoforms were redistributed within the density gradient as a consequence of λ-carrageenan treatment. The approximate halving of the amount of TCEP-R occludin oligomer in fraction 7 was accompanied by decreases in TCEP-R dimeric occludin (from 18% to 12%), 65 kDa monomeric occludin (from 26% to 12%), and 25 kDa LMW occludin (from 58% to 16%). In contrast, no significant changes in either the 53 kDa monomeric occludin isoform or the 35- and 37-kDa LMW occludin isoforms were observed. The approximate 50% reduction in TCEP-R oligomer detected in the 'TJ-associated' lipid raft fraction 7 was mirrored by an approximately two times increase in this oligomeric isoform in fraction 8. Fraction 8 also exhibited increases in the TCEP-R dimer (from 18% to 26%), the 65 kDa monomer (from 27% to 37%), the 53 kDa monomer (from 33% to 45%), 37 kDa LMW isoform (from 33% to 49%), the 35 kDa LMW isoform (from 36% to 55%), and the 25 kDa LMW isoform (from 35% to 84%). In non-raft regions of the density gradient, changes in the relative distribution of TCEP-R dimer and the 65 kDa monomer were also observed following λ-carrageenan treatment. Increased detection of both of these isoforms within the high-density fraction 15 (ρ = 1.168 g/mL) may reflect trafficking of these two occludin isoforms away from plasma membrane lipid raft domains to the cytoplasm. Collectively, this analysis of fractionation data revealed a multiplicity of alterations in the association of different occludin isoforms with lipid raft and non-raft domains and suggests that significant disruption of occludin trafficking and occludin

oligomeric assembly has occurred following the onset of peripheral inflammatory hyperalgesia.

The density gradient data were also analyzed to provide information concerning the relative amounts of different occludin isoforms associated with membrane domains of the same density. The effect of λ-carrageenan treatment on relative occludin isoform composition, within fractions 7, 8, and 10, were determined by calculating the band density for each isoform as a percentage of the sum of band densities for all occludin isoforms detected within the fraction (Fig. 4c). In saline-injected animals, the relative amounts of TCEP-R occludin oligomer and dimer present in fraction 7 were 20.1% and 3.7%, respectively, giving a TCEP-R occludin oligomer/dimer ratio of 5.4. In contrast, the relative amounts of TCEP-R occludin oligomer and dimer present in the higher density fractions 8 and 10 were 12% and 4.6%, and 2.2 and 2.1%, giving TCEP-R occludin oligomer/dimer ratios of 2.6 and 1.4, respectively. λ-Carrageenan treatment altered the relative amounts of TCEP-R occludin oligomer and dimer present in fraction 7 from 20.1% to 9.7% and 3.7% to 4.3%, respectively, decreasing by approximately 50% the TCEP-R occludin oligomer/dimer ratio from 5.4 to 2.3. The relative amounts of TCEP-R occludin oligomer and dimer present in fraction 8 were also altered by λ-carrageenan treatment from 12% to 11% and 4.6% to 6.1%, respectively, which resulted in an approximate 20% reduction of the TCEP-R occludin oligomer/dimer ratio from 2.3 to 1.8. Figure 4d illustrates the inverse relationship between occludin oligomer/dimer (O/D) ratio and fraction density. As the fraction density is decreased, oligomerization is increased. Taken together, these data reveal that within 3 h of inducing peripheral inflammatory pain, significant remodeling of the 'TJ-associated' lipid raft domains at the BBB has occurred such that the bulk of the TCEP-R occludin oligomer is no longer concentrated within tightly-packed, plasma membrane lipid raft domains characterized by a narrowly defined density and a high TCEP-R oligomer/dimer ratio.

λ-Carrageenan modulation of ZO-1 trafficking

Western blots of density gradient fractions from saline-injected, control rats probed for ZO-1 revealed prominent staining for this TJ accessory protein in both plasma membrane lipid rafts and non-raft intracellular compartments (Fig. 5). λ-Carrageenan treatment did not promote noticeable changes in ZO-1 distribution within different plasma membrane lipid raft domains. However, the association of ZO-1 with higher density fractions was markedly decreased.

λ-Carrageenan disrupts occludin oligomeric assembly

To examine in more detail the effect of peripheral inflammatory pain on the relationship between oligomeric, dimeric, and monomeric isoforms of occludin within the 'TJ-associated' low-density plasma membrane lipid raft domain (fraction 7, $\rho = 1.081$ g/mL), equal protein aliquots of fraction 7 were prepared for SDS—PAGE under non-reducing conditions and strongly reducing conditions. Non-reducing conditions involved exposure of samples to 2% SDS and heating to 70 °C for 10 min before electrophoresis; strongly reducing conditions subjected samples to 10% SDS and 10 mM EDT, and heating to 100 °C for 10 min before electrophoresis. Samples from fractionation experiments carried out on different days were electrophoresed on the same gels to ensure identical conditions for both electrophoresis and Western blot analysis. Multiple exposures of Western blots probed with the C-terminus occludin antibody (Zymed 71–1500) were taken to ensure that density measurements for a particular occludin isoform were within the linear range of the film.

In non-reducing blots from saline-injected animals, a substantial amount of oligomeric (> 150 kDa) occludin was detected (Fig. 6a and b). λ-Carrageenan treatment reduced this oligomeric occludin by 35% (Fig. 6c). Non-reducing blots also showed prominent staining for dimeric (*c*. 110–120 kDa) occludin, which was reduced by 26% by peripheral inflammatory

hyperalgesia. Very little monomeric (53 and 65 kDa) occludin was detected in non-reducing blots from saline- or λ-carrageenan-injected animals, suggesting these monomeric isoforms were attached by SDS-resistant, disulfide-bond linkage to higher order oligomeric occludin structures. As expected, treatment with the hydrophobic reducing agent EDT effectively reduced the higher molecular weight oligomeric and dimeric occludin isoforms to the 53 and 65 kDa occludin isoforms, affirming the latter's participation as monomeric building blocks in higher order occludin protein structures. Approximately equivalent amounts of the 53 and 65 kDa monomers were detected in reduced blots prepared from saline-injected animals. Interestingly, λ-carrageenan treatment produced a greater reduction in the 65 kDa (45%) than in the 53 kDa monomer (11%). Collectively, these data affirm that λ-carrageenan treatment significantly disrupted the integrity of occludin oligomeric assemblies within 'TJ-associated' plasma membrane lipid raft domains.

Discussion

In this study, we used detergent-free density gradient fractionation of intact microvessels to investigate the effect of λ-carrageenan-induced peripheral inflammatory pain (i.e., hyperalgesia) on occludin oligomeric complexes within plasma membrane lipid rafts at TJs of the BBB. Reducing SDS—PAGE/Western blot analysis of density gradient fractions treated with the hydrophilic reducing agent TCEP revealed that hind paw injection of λ-carrageenan promoted a marked change in the relative amounts of oligomeric, dimeric, and monomeric isoforms of occludin associated with different plasma membrane lipid raft domains and subcellular compartments of microvascular endothelial cells. Using non-reducing SDS—PAGE to analyze occludin associated with 'TJ-associated' plasma membrane lipid rafts, we found that λ-carrageenan-induced inflammatory pain decreased the amount of total oligomeric occludin (> 150 kDa) by 35%. Our data show a marked disruption of oligomeric occludin at TJs of the BBB takes place within 3 h of the injection of λ-carrageenan in the hind paw of female Sprague—Dawley rats and reveal that disassembly of TJ-associated occludin oligomeric complexes is accompanied by the reduction of intermolecular disulfide bonds.

Previous studies from our laboratory show that injection of λ-carrageenan induced a biphasic response in BBB paracellular permeability over a 72 h time course (Huber *et al*. 2002; Hau *et al*. 2004). Significant change in paracellular permeability was detected as early as 1 h post-injection, and peaks in brain uptake of [^{14}C]sucrose occurred at 3 and 48 h post-injection. The greatest change in permeability was found at 3 h, at which time an approximate 66% increase in paracellular permeability was observed. The observed ability of TJs at the BBB to quickly modulate their restriction of paracellular transport suggested that λ-carrageenan-induced post-translational modifications of key TJ transmembrane and accessory proteins could be invoking conformational changes that were disruptive to the multiprotein TJ complex. Recently, we reported that TJ complexes, isolated from intact cerebral microvessels within the context of their normal plasma membrane lipid raft environment, contain high molecular weight oligomeric assemblies of occludin maintained by disulfide bonds embedded within hydrophobic regions (McCaffrey *et al*. 2007).

Because disulfide bonds not only provide structural support but also a readily reversible means of manipulating protein conformation and function (Hogg 2003; Jordan and Gibbins 2006; Ottaviano *et al*. 2008), we undertook the current study to investigate if peripheral inflammatory pain altered the disulfide-bond integrity of oligomeric occludin complexes at TJs of the BBB *in vivo*. Using density gradient fractionation of cerebral microvessels to isolate membrane domains containing oligomeric occludin complexes, we investigated if 3 h after injection of λ-carrageenan in the rat hind paw, the time of maximum increase in paracellular permeability (Huber *et al*. 2002; Hau *et al*. 2004), there was a change in (i) the density at which oligomeric isoforms of occludin co-localized within an isosmotic OptiPrep gradient, (ii) the sensitivity to

disulfide bond reduction of oligomeric occludin associated with different membrane domains, and (iii) the relative isoform composition of occludin associated with plasma membrane lipid rafts of different density. Increased association of oligomeric occludin with plasma membrane domains of decreased lipid order (i.e., higher density) would imply that distinct changes in the interaction between oligomeric occludin and its lipid environment have occurred, which may affect occludin oligomeric conformation. Increased access of a hydrophilic reducing agent to previously inaccessible disulfide bonds within oligomeric occludin would suggest that conformational changes might have disrupted the tightly packed multiprotein complex. Changes in the relative occludin isoform composition within a membrane domain of particular density would indicate that disassembly of covalently bonded higher order structures has taken place.

Non-reducing SDS—PAGE/Western blot of occludin co-localizing with markers of intact TJs (Rab13 and oligomeric caveolin-1) within the low density 'TJ-associated' plasma membrane lipid rafts (density gradient fraction 7, $\rho = 1.081$ g/mL) of saline-injected animals characteristically revealed very little staining for monomeric (53 and 65 kDa) isoforms and substantial staining for higher molecular weight (> 150 kDa) oligomeric structures. A lesser amount of dimeric occludin (*c*. 100–120 kDa) was typically detected, in addition to a prominent amount of LMW occludin (25 and 35 kDa). Control experiments wherein aliquots of density gradient fraction 7 were treated with the hydrophobic reducing agent EDT reduced essentially all of the oligomeric and dimeric occludin isoforms and significantly increased the monomeric (53 and 65 kDa) isoforms. Because staining for LMW occludin (25, 35, and 37 kDa) was detected in the absence of reducing agent, and increased by EDT-treatment, these isoforms appear to be associated with oligomeric occludin assemblies by either non-covalent, SDS-sensitive interactions and/or disulfide bonds. Treatment of aliquots of density gradient fraction 7 with the hydrophilic reducing agent TCEP revealed that occludin multiprotein assemblies at the TJ contain core oligomeric and dimeric structures that are maintained by disulfide bonds embedded within transmembrane regions. Moreover, prominent staining for monomeric (53 and 65 kDa) occludin isoforms revealed that under normal conditions there is a subset of intermolecular disulfide bonds maintaining occludin oligomeric assemblies that are readily accessible to modification. The TCEP-R oligomer/dimer ratio for occludin associated with a specific gradient fraction can be used as a measure of the relative amounts of hydrophobic disulfide bonds within occludin oligomers. This ratio was found to increase with decreasing fraction density. This suggests that disulfide bond formation between cysteine residues within transmembrane regions was enhanced by an increase in lipid order within plasma membrane lipid rafts. In saline-injected animals, the bulk of oligomeric occludin that was resistant to reduction by TCEP was detected in fraction 7. In λ-carrageenan-injected animals, only 35% of the total amount of oligomeric occludin co-localized at this density, and the effect of λ-carrageenan treatment was to reduce the TCEP-R oligomer/dimer ratio for occludin by approximately twofold.

Combining analysis of our non-reducing and reducing SDS—PAGE/Western blot data for the 'TJ-associated' oligomeric occludin, and the occludin associated with other plasma membrane and intracellular domains led us to hypothesize that λ-carrageenan-induced peripheral inflammatory pain induces a graded disassembly of occludin oligomeric complexes involving sequential increases in disulfide bond reduction. Our data are not inconsistent with a disassembly mechanism of oligomeric occludin complexes within 'TJ-associated' plasma membrane lipid rafts that is initiated by selective reduction of disulfide bonds between cysteine residues within extracellular loops or first transmembrane domains connecting occludin molecules on apposing cell membranes. Conformational changes promoted by relaxation of structural restrictions invoked by disulfide bonds could then lead to altered protein—lipid interactions, and consequently a remodeling of the lipid raft environment. This, in turn, would lead to a decrease in the lipid/protein ratio and an increase in the buoyant density at which these

higher molecular weight occludin isoforms are detected within a density gradient. In this model, disulfide bond reduction within the less tightly packed oligomeric assembly would be enhanced within plasma membrane lipid rafts of higher density. This would increase the extent of dismantling of the oligomeric complex into component dimeric, monomeric, and LMW occludin isoforms. Reducing SDS—PAGE using the hydrophilic reducing agent, TCEP, would be expected to reveal decreases in oligomer to dimer ratios reflecting the increased accessibility of disulfide bonds within oligomeric assemblies to reduction caused by changes in occludin subunit conformation. Our data are in agreement with this and show both an increase in the amount of oligomeric occludin associated with higher density plasma membrane lipid rafts and an increase in dimeric, monomeric, and LMW isoforms relative to oligomeric isoforms within these higher density membrane domains.

Occludin sequence analysis reveals the presence of seven cysteine residues (Fig. 7a). Three of the cysteine residues reside within transmembrane regions, two are present within the second extracellular loop, and two are present within the cytoplasmic C-terminus. All seven cysteine residues are conserved in placental mammals, and all except Cys_{410} and Cys_{501} within the cytoplasmic C-terminus, are conserved in vertebrates as diverse as amphibians, birds, marsupials, rodents, and humans (Lloyd *et al*. 2003). Such conservation requires strong selective pressure during evolution and implies that these cysteine residues play essential role (s) in occludin function. Cysteine residues are also important to claudin-5 function. Mutation of either cysteine in the first extracellular domain abolishes the ability of claudin-5 to increase transepithelial resistance in canine kidney cells (Wen *et al*. 2004).

Computer modeling of rat occludin (UniProtKB/Swiss-Prot entry Q6P6T5) using Disulfind (Ceroni *et al*. 2006) indicates a very low probability that any of the cysteine residues in occludin form intrachain disulfide bonds; however, it does not rule out the possibility that they form interchain disulfide bonds. A hydrophobicity plot (Kyte and Doolittle 1982) constructed for rat occludin (Fig. 7b) shows the relative hydrophobicity of the environment of each cysteine residue and supports the suggestion that side-by-side interaction between the first transmembrane domains of two adjacent occludin molecules could promote disulfide bond(s) between Cys_{76} and/or Cys_{82} to produce dimers insensitive to reduction by a hydrophilic reducing agent such as TCEP. In addition, occludin dimers formed by intermolecular disulfide bond(s) between Cys_{410} and/or Cys_{501} would be expected to be sensitive to reduction by a hydrophilic reducing agent. Interaction between either (or both) of the cysteines present in the second extracellular loop of one occludin molecule (in one cell) with cysteine(s) present within the second extracellular loop of another occludin molecule (in the apposing cell) could promote the formation of an occludin oligomer, if each occludin molecule was already disulfide-bonded to another occludin molecule within the same cell. Moreover, the extreme closeness of adjacent cell plasma membranes at the TJ could promote disulfide-bonded occludin structures through, for example, interactions between a cysteine present within the second extracellular loop of one occludin molecule with Cys_{82} present at the outermost edge of the first transmembrane domain of another occludin molecule. Possible disulfide bond formation between adjacent and apposing occludin molecules is diagrammatically illustrated in Fig. 8.

Numerous *in vitro* studies using peptides homologous to regions of either of the two extracellular loops of occludin have differentially revealed their importance in occludin trafficking to the TJ and maintenance of TJ function (Van Itallie and Anderson 1997; Wong and Gumbiner 1997; Lacaz-Vieira *et al*. 1999; Balda *et al*. 2000; Medina *et al*. 2000; Chung *et al*. 2001; Tavelin *et al*. 2003; Nusrat *et al*. 2005; Everett *et al*. 2006; Tokunaga *et al*. 2007; Jin *et al*. 2008). Thiol disulfide interchanges leading to reduction of protein disulfide bonds within occludin oligomeric assemblies could be catalyzed by oxidoreductases such as protein disulfide isomerase (EC 5.3.4.2) (Edman *et al*. 1985) that are active at the endothelial cell surface (Hotchkiss *et al*. 1998; Swiatkowska *et al*. 2008). Our data support the hypothesis that

disulfide bond modification is a previously unrecognized ‘Achilles heel’ of occludin oligomeric structural integrity that could be therapeutically manipulated to effect changes in paracellular permeability at the BBB.

Acknowledgments

This work was supported by NIH grants R01-NS 39592, R01-NS42652, R01-DA12684 to TPD, and CA 09820-0251 to GM.

Abbreviations used

BBB, blood-brain barrier; EDT, 1,2-ethanedithiol; LMW, low molecular weight; PVDF, polyvinylidene difluoride; SDS—PAGE, sodium dodecyl sulfate—polyacrylamide gel electrophoresis; TCEP, tris (2-carboxyethyl) phosphine hydrochloride; TCEP-R, TCEP-resistant; TJ, tight junction; ZO-1, zonula occludens-1.

References

Andersson J. The inflammatory reflex —0 introduction. J. Intern. Med 2005;257:122–125. [PubMed: 15656871]

Balda MS, Flores-Maldonado C, Cereijido M, Matter K. Multiple domains of occludin are involved in the regulation of paracellular permeability. J. Cell. Biochem 2000;78:85–96. [PubMed: 10797568]

Barrios-Rodiles M, Brown KR, Ozdamar B, et al. High-throughput mapping of a dynamic signaling network in mammalian cells. Science 2005;307:1621–1625. [PubMed: 15761153]

Blasig IE, Winkler L, Lassowski B, et al. On the self-association potential of transmembrane tight junction proteins. Cell. Mol. Life Sci 2006;63:505–514. [PubMed: 16456617]

de Boer AG, Gaillard PJ. Drug targeting to the brain. Annu. Rev. Pharmacol. Toxicol 2007;47:323–355. [PubMed: 16961459]

Brooks TA, Hawkins BT, Huber JD, Egleton RD, Davis TP. Chronic inflammatory pain leads to increased blood-brain barrier permeability and tight junction protein alterations. Am. J. Physiol. Heart Circ. Physiol 2005;289:H738–H743. [PubMed: 15792985]

Brooks TA, Ocheltree SM, Seelbach MJ, Charles RA, Nametz N, Egleton RD, Davis TP. Biphasic cytoarchitecture and functional changes in the BBB induced by chronic inflammatory pain. Brain Res 2006;1120:172–182. [PubMed: 17007822]

Ceroni A, Passerini A, Vullo A, Frasconi P. DISULFIND: a disulfide bonding state and cysteine connectivity prediction server. Nucleic Acids Res 2006;34:W177–W181. [PubMed: 16844986]

Chen YH, Lu Q. Association of nonreceptor tyrosine kinase c-yes with tight junction protein occludin by coimmunoprecipitation assay. Methods Mol. Biol 2003;218:127–132. [PubMed: 12616717]

Chung NP, Mruk D, Mo MY, Lee WM, Cheng CY. A 22-amino acid synthetic peptide corresponding to the second extracellular loop of rat occludin perturbs the blood-testis barrier and disrupts spermatogenesis reversibly in vivo. Biol. Reprod 2001;65:1340–1351. [PubMed: 11673248]

DeMaio L, Rouhanizadeh M, Reddy S, Sevanian A, Hwang J, Hsiai TK. Oxidized phospholipids mediate occludin expression and phosphorylation in vascular endothelial cells. Am. J. Physiol. Heart Circ. Physiol 2006;290:H674–H683. [PubMed: 16172163]

Desai BS, Monahan AJ, Carvey PM, Hendey B. Blood-brain barrier pathology in Alzheimer’s and Parkinson’s disease: implications for drug therapy. Cell Transplant 2007;16:285–299. [PubMed: 17503739]

Dobrogowska DH, Vorbrodt AW. Immunogold localization of tight junctional proteins in normal and osmotically-affected rat blood-brain barrier. J. Mol. Histol 2004;35:529–539. [PubMed: 15571330]

Edman JC, Ellis L, Blacher RW, Roth RA, Rutter WJ. Sequence of protein disulphide isomerase and implications of its relationship to thioredoxin. Nature 1985;317:267–270. [PubMed: 3840230]

Everett RS, Vanhook MK, Barozzi N, Toth I, Johnson LG. Specific modulation of airway epithelial tight junctions by apical application of an occludin peptide. Mol. Pharmacol 2006;69:492–500. [PubMed: 16288084]

Feldman GJ, Mullin JM, Ryan MP. Occludin: structure, function and regulation. Adv. Drug Deliv. Rev 2005;57:883–917. [PubMed: 15820558]

Fischer S, Wiesnet M, Renz D, Schaper W. H2O2 induces paracellular permeability of porcine brain-derived microvascular endothelial cells by activation of the p44/42 MAP kinase pathway. Eur. J. Cell Biol 2005;84:687–697. [PubMed: 16106912]

Forster C. Tight junctions and the modulation of barrier function in disease. Histochem. Cell Biol 2008;130:55–70. [PubMed: 18415116]

Furuse M, Itoh M, Hirase T, Nagafuchi A, Yonemura S, Tsukita S, Tsukita S. Direct association of occludin with ZO-1 and its possible involvement in the localization of occludin at tight junctions. J. Cell Biol 1994;127:1617–1626. [PubMed: 7798316]

Gonzalez-Mariscal L, Tapia R, Chamorro D. Crosstalk of tight junction components with signaling pathways. Biochim. Biophys. Acta 2008;1778:729–756. [PubMed: 17950242]

Hansson E, Zugner R. Can chronic pain and spreading of pain be induced via glial mechanisms? New hypotheses on the generators maintaining protracted pain conditions. Lakartidningen 2005;102:3552, 3555–3556, 3558. [PubMed: 16408393]

Hargreaves K, Dubner R, Brown F, Flores C, Joris J. A new and sensitive method for measuring thermal nociception in cutaneous hyperalgesia. Pain 1988;32:77–88. [PubMed: 3340425]

Harhaj NS, Antonetti DA. Regulation of tight junctions and loss of barrier function in pathophysiology. Int. J. Biochem. Cell Biol 2004;36:1206–1237. [PubMed: 15109567]

Hau VS, Huber JD, Campos CR, Davis RT, Davis TP. Effect of lambda-carrageenan-induced inflammatory pain on brain uptake of codeine and antinociception. Brain Res 2004;1018:257–264. [PubMed: 15276886]

Hawkins BT, Davis TP. The blood-brain barrier/neurovascular unit in health and disease. Pharmacol. Rev 2005;57:173–185. [PubMed: 15914466]

Hendset M, Haslemo T, Rudberg I, Refsum H, Molden E. The complexity of active metabolites in therapeutic drug monitoring of psychotropic drugs. Pharmacopsychiatry 2006;39:121–127. [PubMed: 16871467]

Hirase T, Kawashima S, Wong EY, Ueyama T, Rikitake Y, Tsukita S, Yokoyama M, Staddon JM. Regulation of tight junction permeability and occludin phosphorylation by Rhoa-p160ROCK-dependent and -independent mechanisms. J. Biol. Chem 2001;276:10423–10431. [PubMed: 11139571]

Hogg PJ. Disulfide bonds as switches for protein function. Trends Biochem. Sci 2003;28:210–214. [PubMed: 12713905]

Hotchkiss KA, Matthias LJ, Hogg PJ. Exposure of the cryptic Arg-Gly-Asp sequence in thrombospondin-1 by protein disulfide isomerase. Biochim. Biophys. Acta 1998;1388:478–488. [PubMed: 9858782]

Huber JD, Witt KA, Hom S, Egleton RD, Mark KS, Davis TP. Inflammatory pain alters blood-brain barrier permeability and tight junctional protein expression. Am. J. Physiol. Heart Circ. Physiol 2001;280:H1241–H1248. [PubMed: 11179069]

Huber JD, Hau VS, Borg L, Campos CR, Egleton RD, Davis TP. Blood-brain barrier tight junctions are altered during a 72-h exposure to lambda-carrageenan-induced inflammatory pain. Am. J. Physiol. Heart Circ. Physiol 2002;283:H1531–H1537. [PubMed: 12234806]

Huber JD, Campos CR, Mark KS, Davis TP. Alterations in blood-brain barrier ICAM-1 expression and brain microglial activation after lambda-carrageenan-induced inflammatory pain. Am. J. Physiol. Heart Circ. Physiol 2006;290:H732–H740. [PubMed: 16199477]

Ibuki T, Matsumura K, Yamazaki Y, Nozaki T, Tanaka Y, Kobayashi S. Cyclooxygenase-2 is induced in the endothelial cells throughout the central nervous system during carrageenan-induced hind paw inflammation; its possible role in hyperalgesia. J. Neurochem 2003;86:318–328. [PubMed: 12871573]

Jin Y, Uchida I, Eto K, Kitano T, Abe S. Size-selective junctional barrier and Ca(2+)-independent cell adhesion in the testis of *Cynops pyrrhogaster*: expression and function of occludin. Mol. Reprod. Dev 2008;75:202–216. [PubMed: 17342736]

Jordan PA, Gibbins JM. Extracellular disulfide exchange and the regulation of cellular function. Antioxid. Redox Signal 2006;8:312–324. [PubMed: 16677077]

Kago T, Takagi N, Date I, Takenaga Y, Takagi K, Takeo S. Cerebral ischemia enhances tyrosine phosphorylation of occludin in brain capillaries. Biochem. Biophys. Res. Commun 2006;339:1197–1203. [PubMed: 16338221]

Kaur C, Ling EA. Blood brain barrier in hypoxic-ischemic conditions. Curr. Neurovasc. Res 2008;5:71–81. [PubMed: 18289024]

Kevil CG, Oshima T, Alexander B, Coe LL, Alexander JS. H_2O_2-mediated permeability: role of MAPK and occludin. Am. J. Physiol. Cell Physiol 2000;279:C21–C30. [PubMed: 10898713]

Krause G, Winkler L, Mueller SL, Haseloff RF, Piontek J, Blasig IE. Structure and function of claudins. Biochim. Biophys. Acta 2008;1778:631–645. [PubMed: 18036336]

Krizbai IA, Bauer H, Bresgen N, Eckl PM, Farkas A, Szatmari E, Traweger A, Wejksza K, Bauer HC. Effect of oxidative stress on the junctional proteins of cultured cerebral endothelial cells. Cell. Mol. Neurobiol 2005;25:129–139. [PubMed: 15962510]

Kyte J, Doolittle RF. A simple method for displaying the hydropathic character of a protein. J. Mol. Biol 1982;157:105–132. [PubMed: 7108955]

Lacaz-Vieira F, Jaeger MM, Farshori P, Kachar B. Small synthetic peptides homologous to segments of the first external loop of occludin impair tight junction resealing. J. Membr. Biol 1999;168:289–297. [PubMed: 10191363]

Lapierre LA, Tuma PL, Navarre J, Goldenring JR, Anderson JM. VAP-33 localizes to both an intracellular vesicle population and with occludin at the tight junction. J. Cell Sci 1999;112(Pt 21):3723–3732. [PubMed: 10523508]

Lloyd RV, Vidal S, Horvath E, Kovacs K, Scheithauer B. Angiogenesis in normal and neoplastic pituitary tissues. Microsc. Res. Tech 2003;60:244–250. [PubMed: 12539179]

Macdonald JL, Pike LJ. A simplified method for the preparation of detergent-free lipid rafts. J. Lipid Res 2005;46:1061–1067. [PubMed: 15722565]

McCaffrey G, Staatz WD, Quigley CA, Nametz N, Seelbach MJ, Campos CR, Brooks TA, Egleton RD, Davis TP. Tight junctions contain oligomeric protein assembly critical for maintaining blood-brain barrier integrity in vivo. J. Neurochem 2007;103:2540–2555.

McKenzie JA, Ridley AJ. Roles of Rho/ROCK and MLCK in TNF-alpha-induced changes in endothelial morphology and permeability. J. Cell. Physiol 2007;213:221–228. [PubMed: 17476691]

Medina R, Rahner C, Mitic LL, Anderson JM, Van Itallie CM. Occludin localization at the tight junction requires the second extracellular loop. J. Membr. Biol 2000;178:235–247. [PubMed: 11140279]

Meyer TN, Schwesinger C, Ye J, Denker BM, Nigam SK. Reassembly of the tight junction after oxidative stress depends on tyrosine kinase activity. J. Biol. Chem 2001;276:22048–22055. [PubMed: 11294856]

Morimoto S, Nishimura N, Terai T, et al. Rab13 mediates the continuous endocytic recycling of occludin to the cell surface. J. Biol. Chem 2005;280:2220–2228. [PubMed: 15528189]

Neuwelt E, Abbott NJ, Abrey L, et al. Strategies to advance translational research into brain barriers. Lancet Neurol 2008;7:84–96. [PubMed: 18093565]

Nusrat A, Chen JA, Foley CS, Liang TW, Tom J, Cromwell M, Quan C, Mrsny RJ. The coiled-coil domain of occludin can act to organize structural and functional elements of the epithelial tight junction. J. Biol. Chem 2000a;275:29816–29822. [PubMed: 10887180]

Nusrat A, Parkos CA, Verkade P, Foley CS, Liang TW, Innis-Whitehouse W, Eastburn KK, Madara JL. Tight junctions are membrane microdomains. J. Cell Sci 2000b;113(Pt 10):1771–1781. [PubMed: 10769208]

Nusrat A, Brown GT, Tom J, Drake A, Bui TT, Quan C, Mrsny RJ. Multiple protein interactions involving proposed extracellular loop domains of the tight junction protein occludin. Mol. Biol. Cell 2005;16:1725–1734. [PubMed: 15659655]

Ottaviano FG, Handy DE, Loscalzo J. Redox regulation in the extracellular environment. Circ. J 2008;72:1–16. [PubMed: 18159092]

Ozdamar B, Bose R, Barrios-Rodiles M, Wang HR, Zhang Y, Wrana JL. Regulation of the polarity protein Par6 by TGFbeta receptors controls epithelial cell plasticity. Science 2005;307:1603–1609. [PubMed: 15761148]

Pan W, Kastin AJ. Tumor necrosis factor and stroke: role of the blood-brain barrier. Prog. Neurobiol 2007;83:363–374. [PubMed: 17913328]

Paris L, Tonutti L, Vannini C, Bazzoni G. Structural organization of the tight junctions. Biochim. Biophys. Acta 2008;1778:646–659. [PubMed: 17945185]

Persidsky Y, Heilman D, Haorah J, Zelivyanskaya M, Persidsky R, Weber GA, Shimokawa H, Kaibuchi K, Ikezu T. Rho-mediated regulation of tight junctions during monocyte migration across the blood-brain barrier in HIV-1 encephalitis (HIVE). Blood 2006;107:4770–4780. [PubMed: 16478881]

Petty MA, Lo EH. Junctional complexes of the blood-brain barrier: permeability changes in neuroinflammation. Prog. Neurobiol 2002;68:311–323. [PubMed: 12531232]

Piontek J, Winkler L, Wolburg H, Muller SL, Zuleger N, Piehl C, Wiesner B, Krause G, Blasig IE. Formation of tight junction: determinants of homophilic interaction between classic claudins. FASEB J 2008;22:146–158. [PubMed: 17761522]

Rao RK, Basuroy S, Rao VU, Karnaky KJ Jr, Gupta A. Tyrosine phosphorylation and dissociation of occludin-ZO-1 and E-cadherin-beta-catenin complexes from the cytoskeleton by oxidative stress. Biochem. J 2002;368:471–481. [PubMed: 12169098]

Reese TS, Karnovsky MJ. Fine structural localization of a blood-brain barrier to exogenous peroxidase. J. Cell Biol 1967;34:207–217. [PubMed: 6033532]

Rost B, Yachdav G, Liu J. The PredictProtein server. Nucleic Acids Res 2004;32:321–326.

Rudajev V, Novotny J, Hejnova L, Milligan G, Svoboda P. Dominant portion of thyrotropin-releasing hormone receptor is excluded from lipid domains. Detergent-resistant and detergent-sensitive pools of TRH receptor and Gqalpha/G11alpha protein. J. Biochem. (Tokyo) 2005;138:111–125. [PubMed: 16091585]

Sanchez-Pulido L, Martin-Belmonte F, Valencia A, Alonso MA. MARVEL: a conserved domain involved in membrane apposition events. Trends Biochem. Sci 2002;27:599–601. [PubMed: 12468223]

Seelbach MJ, Brooks TA, Egleton RD, Davis TP. Peripheral inflammatory hyperalgesia modulates morphine delivery to the brain: a role for P-glycoprotein. J. Neurochem 2007;102:1677–1690. [PubMed: 17697052]

Seth A, Sheth P, Elias BC, Rao R. Protein phosphatases 2A and 1 interact with occludin and negatively regulate the assembly of tight junctions in the CACO-2 cell monolayer. J. Biol. Chem 2007;282:11487–11498. [PubMed: 17298946]

Sheth P, Basuroy S, Li C, Naren AP, Rao RK. Role of phosphatidylinositol 3-kinase in oxidative stress-induced disruption of tight junctions. J. Biol. Chem 2003;278:49239–49245. [PubMed: 14500730]

Stamatovic SM, Dimitrijevic OB, Keep RF, Andjelkovic AV. Protein kinase Calpha-RhoA cross-talk in CCL2-induced alterations in brain endothelial permeability. J. Biol. Chem 2006;281:8379–8388. [PubMed: 16439355]

Swiatkowska M, Szymanski J, Padula G, Cierniewski CS. Interaction and functional association of protein disulfide isomerase with alpha(V)beta(3) integrin on endothelial cells. FEBS J 2008;275:1813–1823. [PubMed: 18331351]

Tavelin S, Hashimoto K, Malkinson J, Lazorova L, Toth I, Artursson P. A new principle for tight junction modulation based on occludin peptides. Mol. Pharmacol 2003;64:1530–1540. [PubMed: 14645684]

Tokunaga Y, Kojima T, Osanai M, Murata M, Chiba H, Tobioka H, Sawada N. A novel monoclonal antibody against the second extracellular loop of occludin disrupts epithelial cell polarity. J. Histochem. Cytochem 2007;55:735–744. [PubMed: 17371936]

Van Itallie CM, Anderson JM. Occludin confers adhesiveness when expressed in fibroblasts. J. Cell Sci 1997;110(Pt 9):1113–1121. [PubMed: 9175707]

Vandenbroucke E, Mehta D, Minshall R, Malik AB. Regulation of endothelial junctional permeability. Ann. N Y Acad. Sci 2008;1123:134–145. [PubMed: 18375586]

Vorbrodt AW, Dobrogowska DH. Molecular anatomy of interendothelial junctions in human blood-brain barrier microvessels. Folia Histochem. Cytobiol 2004;42:67–75. [PubMed: 15253128]

Watkins LR, Maier SF. The pain of being sick: implications of immune-to-brain communication for understanding pain. Annu. Rev. Psychol 2000;51:29–57. [PubMed: 10751964]

Watkins LR, Maier SF. Immune regulation of central nervous system functions: from sickness responses to pathological pain. J. Intern. Med 2005;257:139–155. [PubMed: 15656873]

Watkins LR, Maier SF, Goehler LE. Cytokine-to-brain communication: a review and analysis of alternative mechanisms. Life Sci 1995;57:1011–1026. [PubMed: 7658909]

Wen H, Watry DD, Marcondes MC, Fox HS. Selective decrease in paracellular conductance of tight junctions: role of the first extracellular domain of claudin-5. Mol. Cell. Biol 2004;24:8408–8417. [PubMed: 15367662]

Wieseler-Frank J, Maier SF, Watkins LR. Central proinflammatory cytokines and pain enhancement. Neurosignals 2005a;14:166–174. [PubMed: 16215299]

Wieseler-Frank J, Maier SF, Watkins LR. Immune-to-brain communication dynamically modulates pain: physiological and pathological consequences. Brain Behav. Immun 2005b;19:104–111. [PubMed: 15664782]

Wolka AM, Huber JD, Davis TP. Pain and the blood-brain barrier: obstacles to drug delivery. Adv. Drug Deliv. Rev 2003;55:987–1006. [PubMed: 12935941]

Wong V, Gumbiner BM. A synthetic peptide corresponding to the extracellular domain of occludin perturbs the tight junction permeability barrier. J. Cell Biol 1997;136:399–409. [PubMed: 9015310]

Xu Y, Gong B, Yang Y, Awasthi YC, Woods M, Boor PJ. Glutathione-S-transferase protects against oxidative injury of endothelial cell tight junctions. Endothelium 2007;14:333–343. [PubMed: 18080870]

Yamamoto M, Ramirez SH, Sato S, Kiyota T, Cerny RL, Kaibuchi K, Persidsky Y, Ikezu T. Phosphorylation of claudin-5 and occludin by rho kinase in brain endothelial cells. Am. J. Pathol 2008;172:521–533. [PubMed: 18187566]

Zlokovic BV. The blood-brain barrier in health and chronic neurodegenerative disorders. Neuron 2008;57:178–201. [PubMed: 18215617]

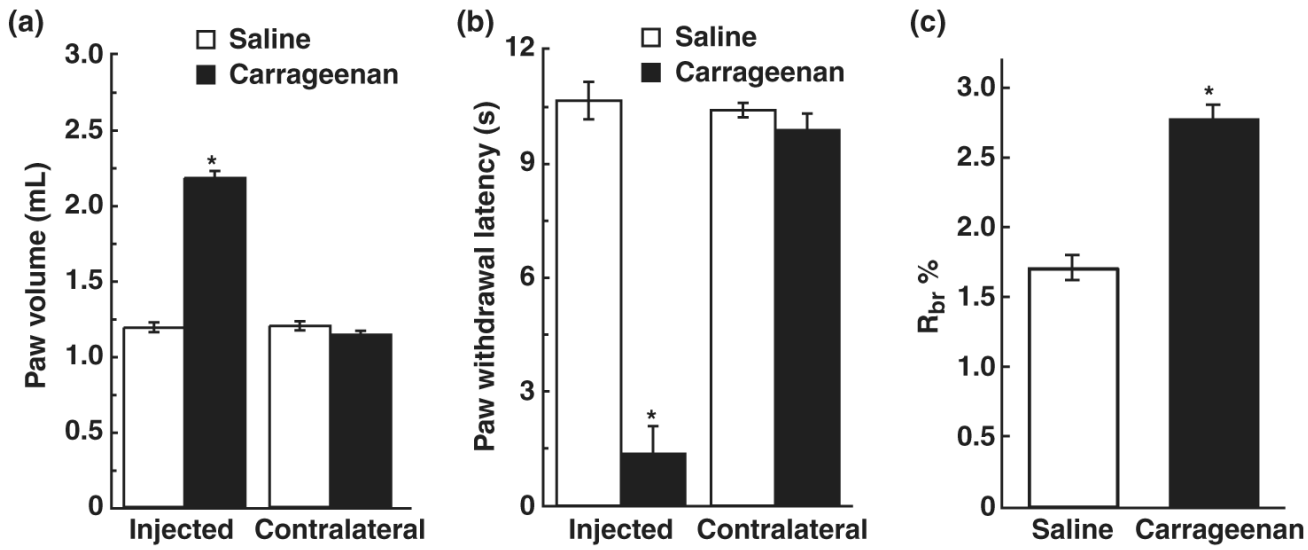

Fig. 1.

λ-Carrageenan induces paw edema, thermal hyperalgesia, and increased permeability at the blood-brain barrier (BBB). Female Sprague—Dawley rats received either vehicle (0.9% saline) or λ-carrageenan (3% in 0.9% saline) into their right hind paws. Three hour post-injection, paw edema was determined by plesmythmography, and paw withdrawal latency was measured by the Hargreaves radiant heat test. Hind paw injection of λ-carrageenan produced significant changes in (a) paw edema, (b) paw withdrawal latency, and (c) R_{br} % ([^{14}C]sucrose permeability). No changes were evident in either the contralateral paw of λ-carrageenan-injected animals or in the hind paws of saline-injected animals. Bar graphs show mean ± SE; $n \geq 10$ per group, *$p < 0.001$ versus treatment groups.

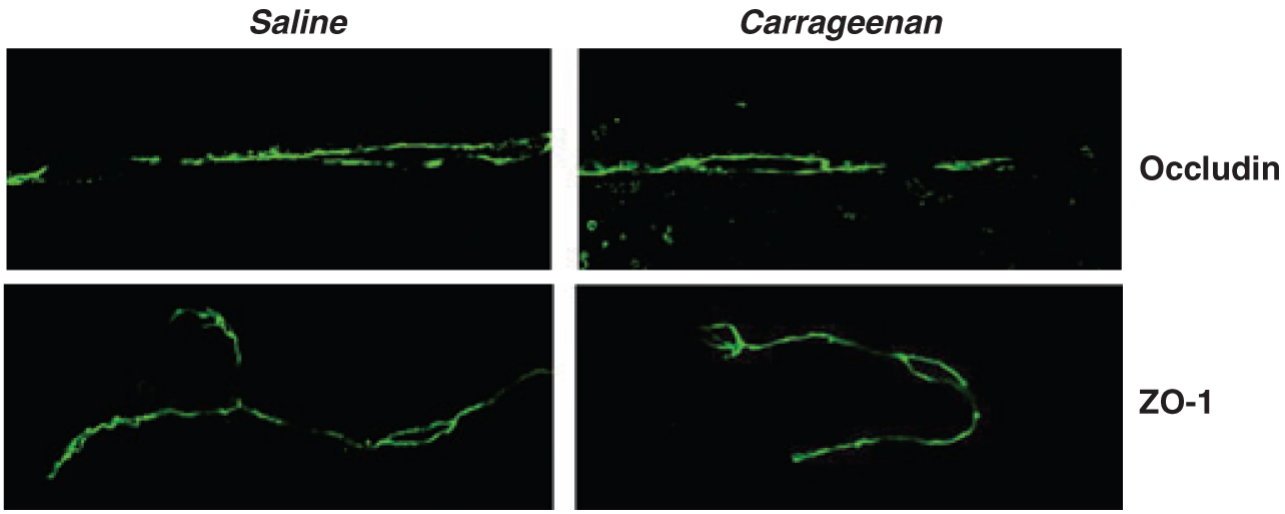

Fig. 2.

λ-Carrageenan modulation of occludin and zonula occludens-1 (ZO-1) localization. Cerebral microvessels prepared from brains from either saline- or λ-carrageenan-injected rats were isolated and imaged by confocal microscopy following immunostaining for occludin and ZO-1. Data shown are representative of two independent experiments (n = 10 rats).

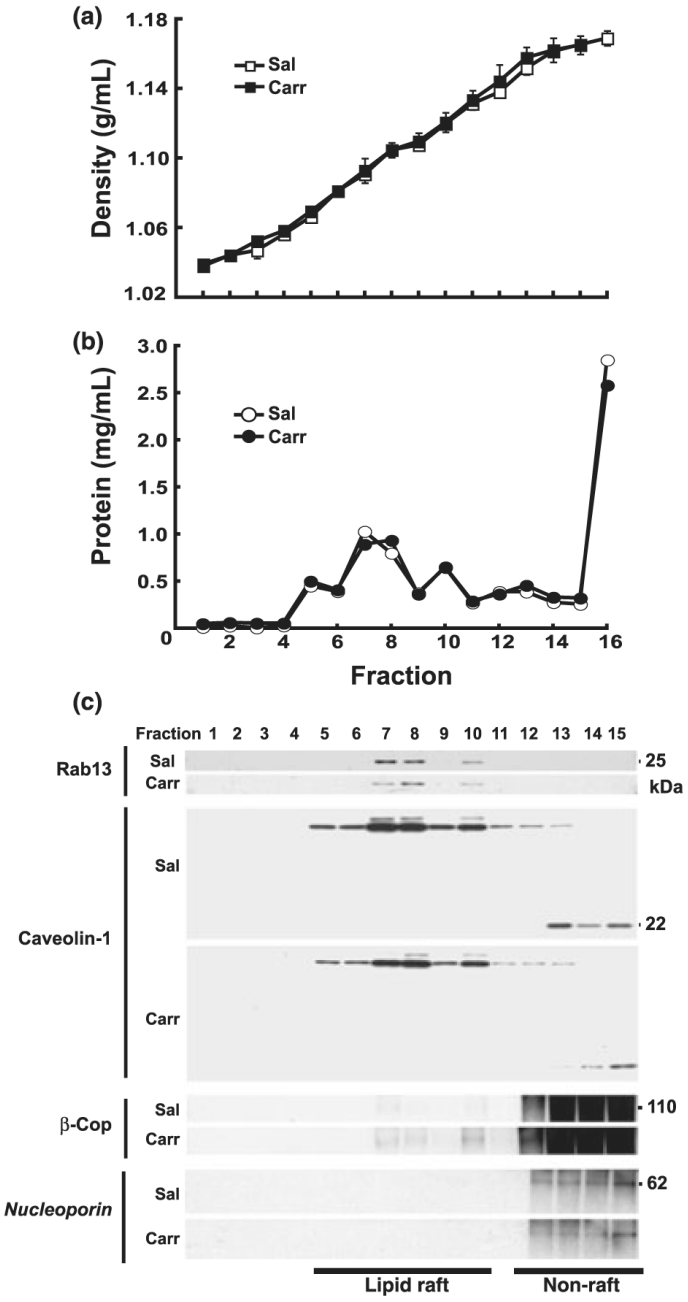

Fig. 3.

Characterization of density gradients for the fractionation of cerebral microvessels. Rat cerebral microvessels prepared from brains from either saline- or λ-carrageenan-injected animals were homogenized in a neutral pH, detergent-free buffer (containing $MgCl_2$ and $CaCl_2$) and fractionated in a discontinuous 0–20% OptiPrep gradient (in the absence of $MgCl_2$ and $CaCl_2$). One-millilitre fractions were collected from the top of the gradient. (a) Mean densities and standard errors from three separate gradients (per animal treatment) on different days (n = 15 rats). (b) Distribution of protein across a representative gradient. (c) Western blots of the first 15 fractions from a representative gradient (for each animal treatment) probed for plasma membrane lipid raft markers (Rab13 and caveolin-1), the Golgi membrane

protein, β-COP, and the nuclear membrane protein, nucleoporin. Bars at the bottom of the figure indicate the distribution of lipid raft and non-raft markers on the gradient. Data shown are representative of at least two independent experiments (n = 10–15 rats) for each treatment condition. Sal, saline; Carr, carrageenan.

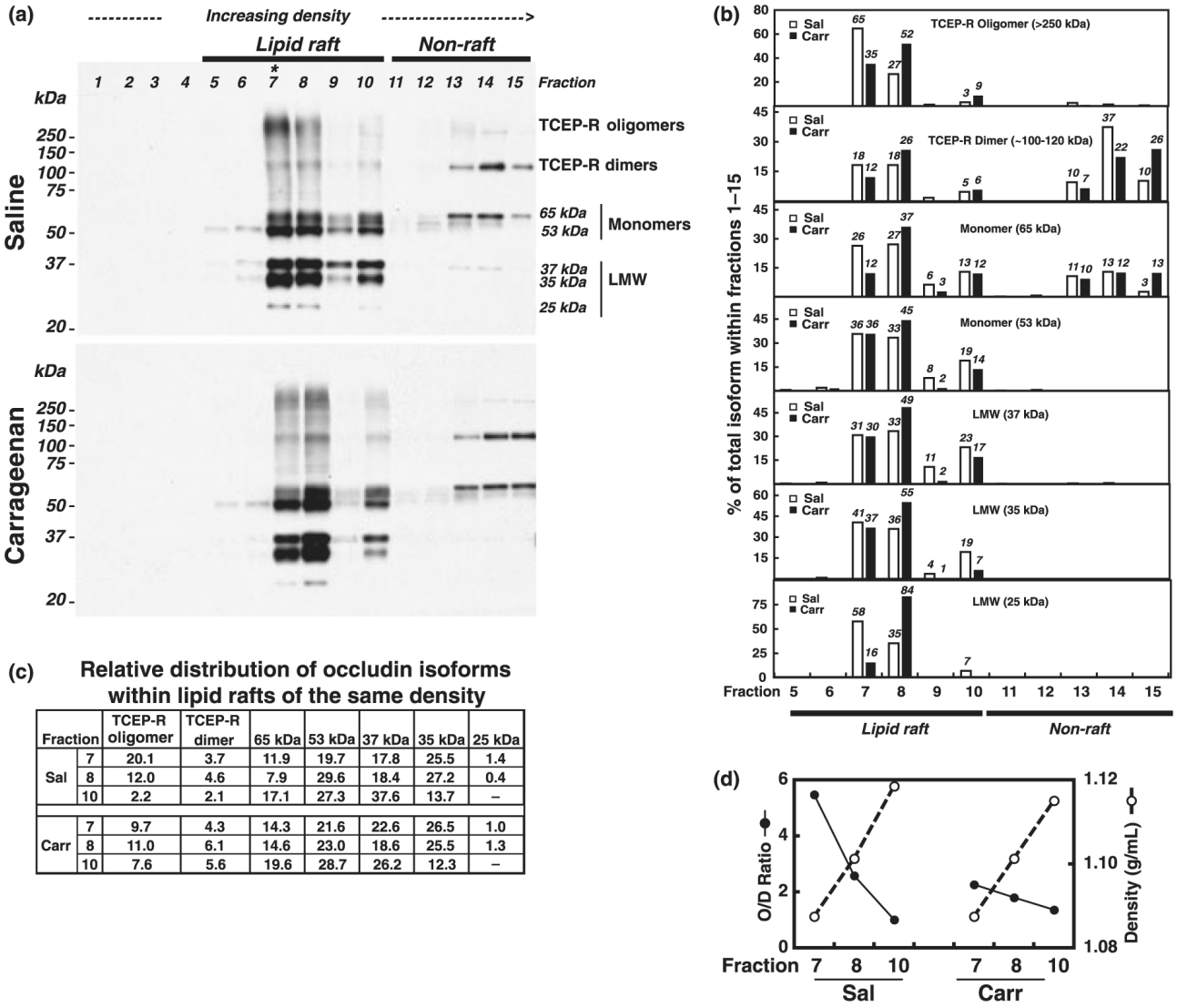

(c) **Relative distribution of occludin isoforms within lipid rafts of the same density**

	Fraction	TCEP-R oligomer	TCEP-R dimer	65 kDa	53 kDa	37 kDa	35 kDa	25 kDa
Sal	7	20.1	3.7	11.9	19.7	17.8	25.5	1.4
	8	12.0	4.6	7.9	29.6	18.4	27.2	0.4
	10	2.2	2.1	17.1	27.3	37.6	13.7	–
Carr	7	9.7	4.3	14.3	21.6	22.6	26.5	1.0
	8	11.0	6.1	14.6	23.0	18.6	25.5	1.3
	10	7.6	5.6	19.6	28.7	26.2	12.3	–

Fig. 4.

λ-Carrageenan modulation of occludin trafficking. Rat cerebral microvessels prepared from brains from either saline-injected or λ-carrageenan-injected animals were homogenized in a neutral pH, detergent-free buffer (containing $MgCl_2$ and $CaCl_2$) and fractionated in a discontinuous 0–20% OptiPrep gradient (in the absence of $MgCl_2$ and $CaCl_2$). One-millilitre fractions were collected from the top of the gradient. (a) Western blots of the first 15 fractions from a representative gradient (for each animal treatment) probed for occludin. Samples were electrophoresed in the presence of 2% sodium dodecyl sulfate and the hydrophilic reducing agent, tris (2-carboxyethyl) phosphine hydrochloride (TCEP), to determine relative distribution of TCEP-resistant (TCEP-R) occludin isoforms. Bars at the top of the figure indicate the distribution of lipid raft and non-raft markers on the gradient. (b) Histograms showing relative distribution, for each animal treatment, of each type of occludin isoform calculated as a percentage of the total band density for that isoform across the gradient. (c) Relative amounts of occludin isoforms detected in fractions 7 and 8, for each animal treatment, calculated as a percentage of the sum of band densities for all isoforms within the same fraction.

(d) Graphs showing relationship between fraction density (open circles) and TCEP-R occludin oligomer/dimer ratio (closed circles) calculated for fractions 7, 8, and 10. Data shown are representative of three independent experiments (n = 15 rats) for each treatment condition. LMW, low molecular weight; Sal, saline; Carr, carrageenan.

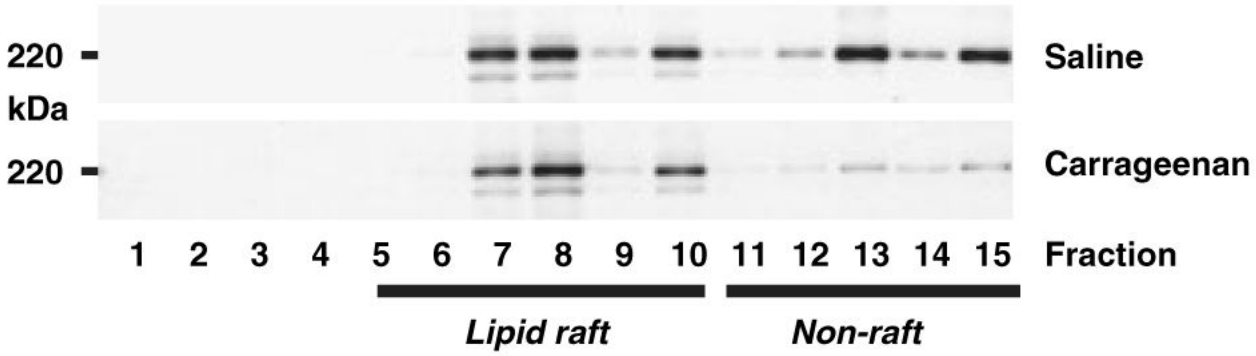

Fig. 5.

λ-Carrageenan alters zonula occludens-1 (ZO-1) trafficking. Rat cerebral microvessels prepared from brains from either saline-injected or λ-carrageenan-injected animals were homogenized in a neutral pH, detergent-free buffer (containing $MgCl_2$ and $CaCl_2$) and fractionated in a discontinuous 0–20% OptiPrep gradient (in the absence of $MgCl_2$ and $CaCl_2$). One-millilitre fractions were collected from the top of the gradient. Western blots of the first 15 fractions from a representative gradient (for each animal treatment) probed for ZO-1. Bars at the bottom of the figure indicate the distribution of lipid raft and non-raft markers on the gradient. Data shown are representative of three independent experiments (n = 15 rats) for each treatment condition.

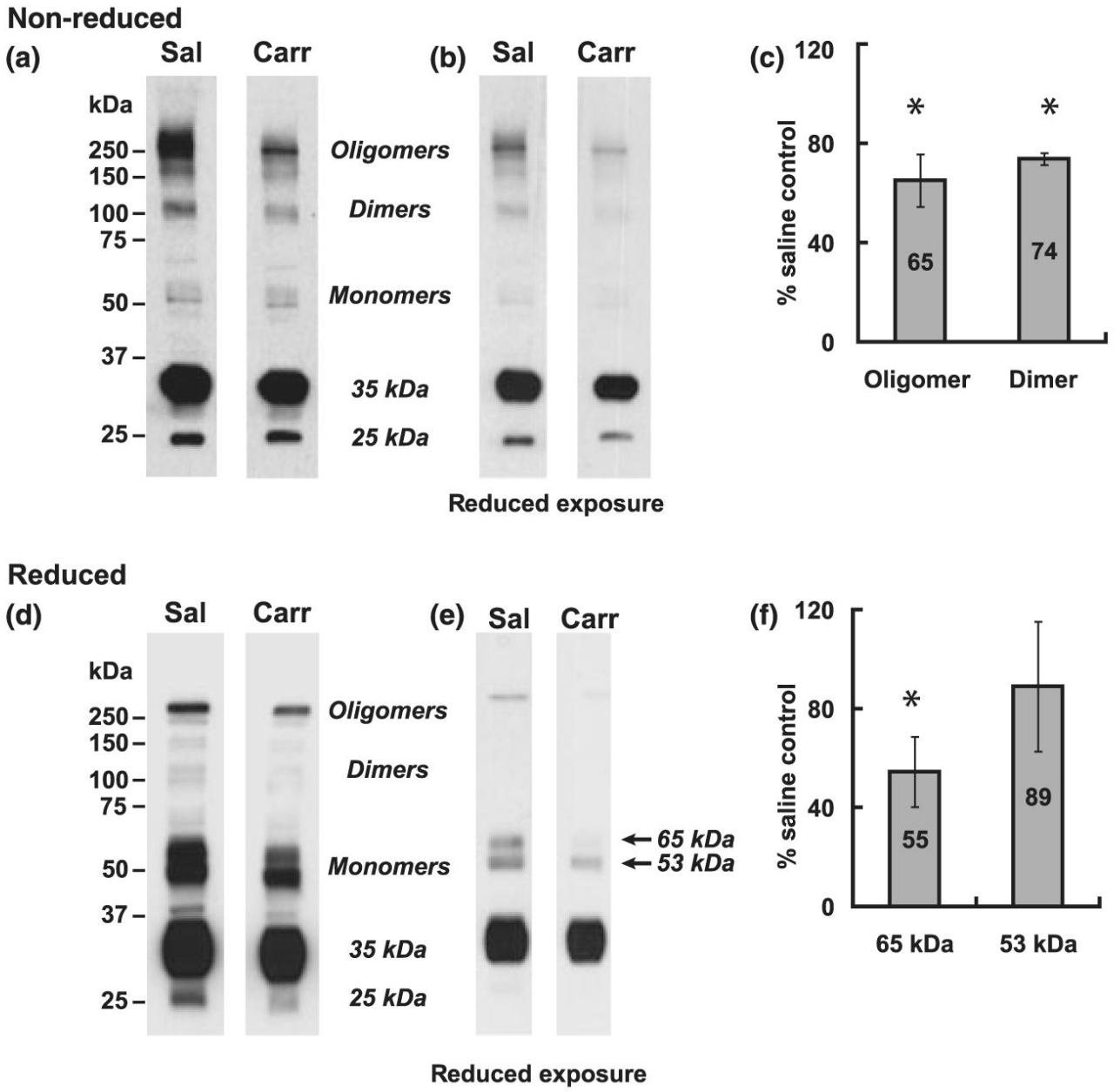

Fig. 6.

λ-Carrageenan disrupts occludin oligomeric assembly. Rat cerebral microvessels prepared from brains from either saline-injected or λ-carrageenan-injected animals were homogenized in a neutral pH, detergent-free buffer (containing $MgCl_2$ and $CaCl_2$) and fractionated in a discontinuous 0–20% OptiPrep gradient (in the absence of $MgCl_2$ and $CaCl_2$). Equal aliquots of fraction 7 were subjected to sodium dodecyl sulfate—polyacrylamide gel electrophoresis (SDS—PAGE) under (a) non-reducing conditions (2% SDS, heated to 70 °C for 10 min before electrophoresis), or (c) strongly reducing conditions (10% SDS, 10 mM 1,2-ethanedithiol heated to 100 °C for 10 min before electrophoresis). Western blots were probed for occludin. Figures b and d are reduced exposures of Fig. (a) and (c), respectively. Ponceau staining for total protein of Western blots was carried out prior to probing with antibody, as a loading control. Data shown are representative of three independent experiments (n = 15 rats) for each

treatment condition. Histograms represent percent change in band density relative to saline-injected controls and are averaged from three independent experiments, *$p < 0.05$. Sal, saline; Carr, carrageenan.

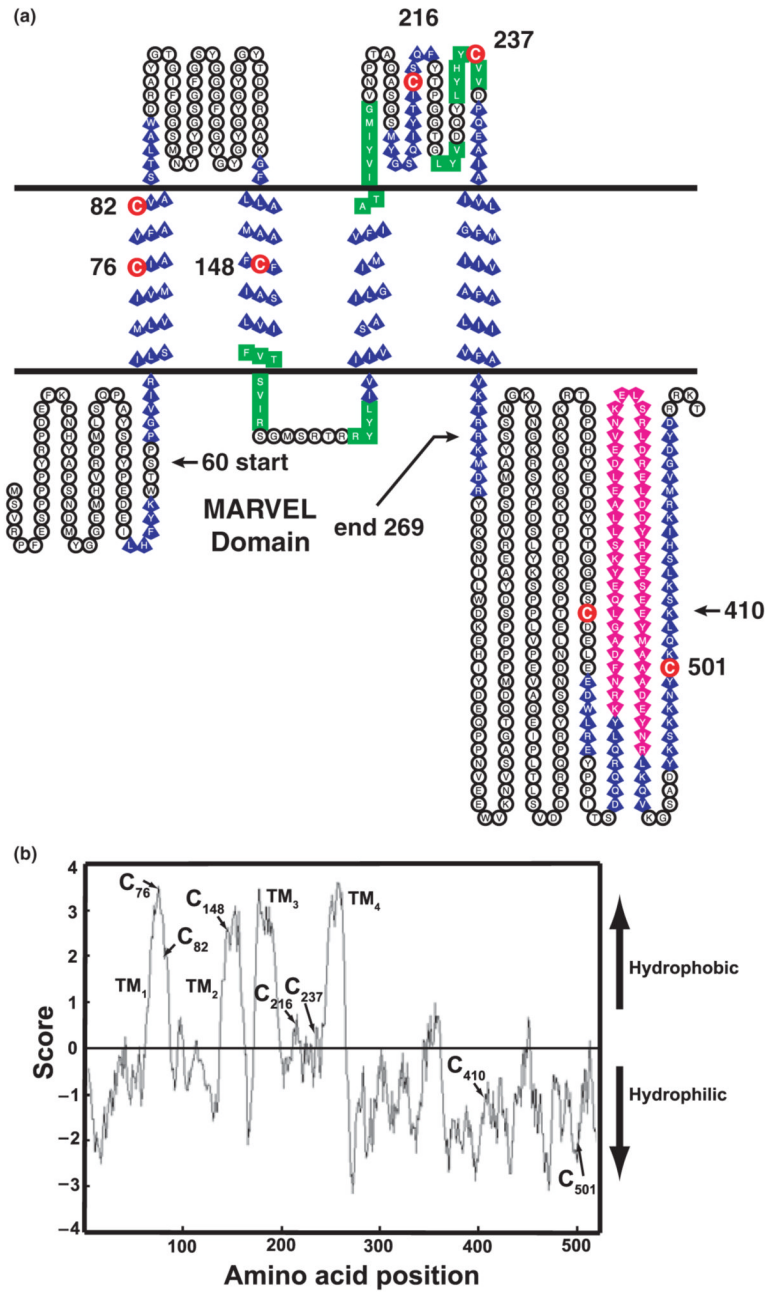

Fig. 7.

Occludin structure. (a) The UniProtKB/Swiss-Prot entry Q6P6T5 for rat occludin, combined with data output from the PredictProtein server (Rost *et al*. 2004), was used to create a TOPO diagram (http://www.sacs.ucsf.edu/TOPO2) in which the alpha helical domains are in blue, the coiled-coil domain is in pink, and extended domains (sheets) are in green. Cysteine residues are marked by red circles and numbers to indicate amino acid location. (b) Kyte–Doolittle hydrophobicity plot of rat occludin shows positions of cysteine residues and their relative hydrophobicity. MARVEL, myelin and lymphocyte and related proteins for vesicle trafficking and membrane link domain.

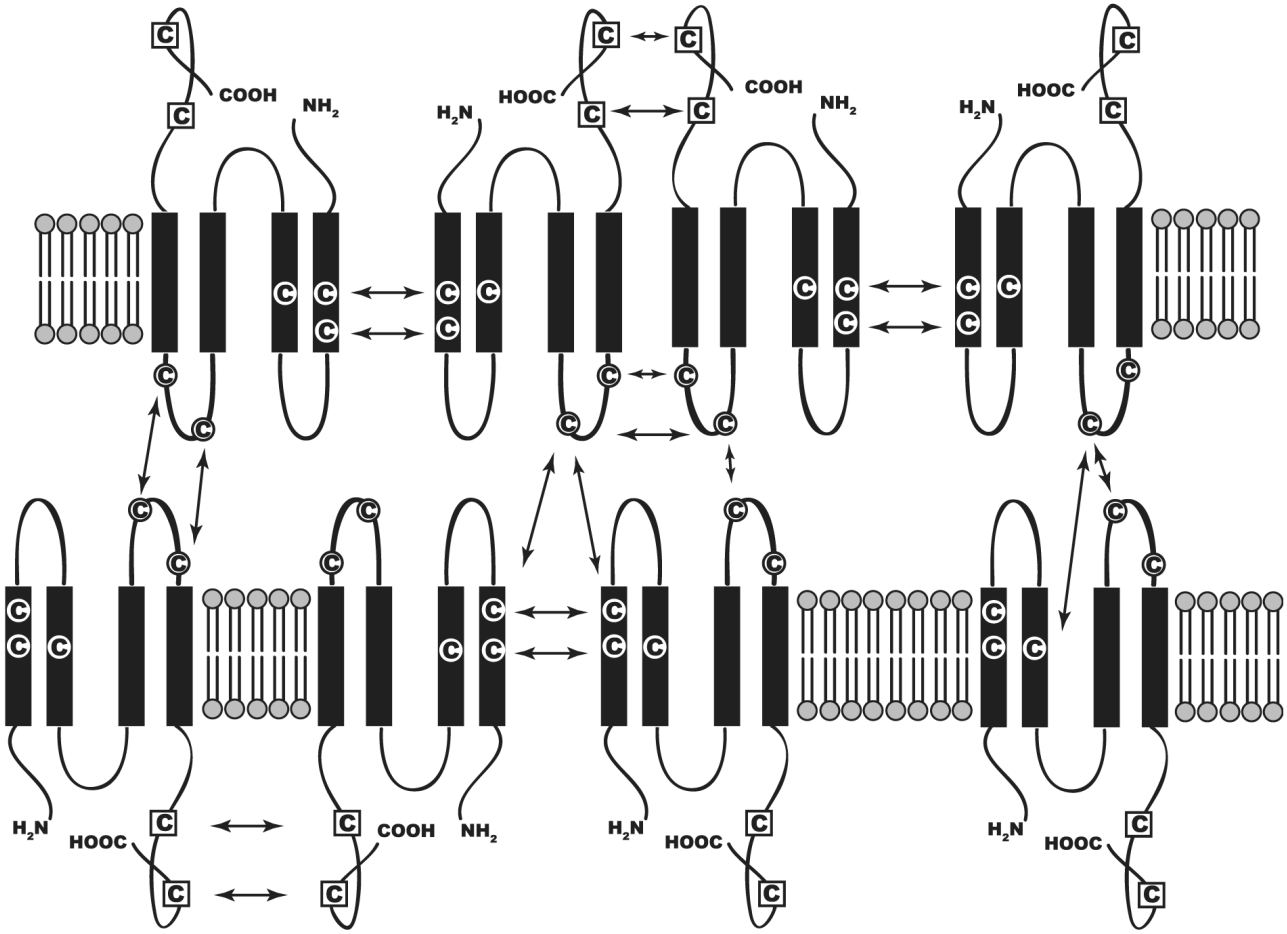

Fig. 8.

Proposed model of occludin disulfide bonds. Occludin monomers show position of conserved cysteine residues (encircled) within the first and second transmembrane domains and the second extracellular loop. Arrows indicate hypothetical disulfide bonds between occludin molecules.